ELECTRICAL FLUCTUATIONS IN SMALL SYSTEMS

José A. Fornés
Universidade Federal de Goiás, Goiânia, GO, Brazil

INTRODUCTION

The importance of local field fluctuations in biological systems has been raised by several authors: Weaver and Astumian (1) presented a calculation of the effects of weak fields on cells. Procopio and Fornés (2), using the fluctuation–dissipation theorem (FDT), presented a calculation of the voltage fluctuations across cell membranes. Protonic fluctuations could be the cause of the dielectric increment of proteins in solution (3, 4). For fluctuations of ion distribution in colloid and polyelectrolyte solutions, see, for instance, (5–9). Local fluctuations can also influence chemical reactions (10). Oosawa (11) calculated that the magnitude of fluctuating voltage and field across different points of an electrolyte solution constituted of point ions using the method of the mode expansion (5, 6, 12–14).

To estimate the electrical fluctuations in small systems, we have to know the electrical capacitance that emerges as a consequence of the processes or by the proper interfaces in the systems (15) e.g., protonation–deprotonation equilibrium at interfaces and in the bulk, the fluctuation of the ionic atmosphere surrounding a charged surface or macroion in an electrolyte solution, also the cell and the inner mitochondrial membranes and the ionic channels, can be well represented by combinations of resistances and capacitances, etc. The electrical capacitance is the link to the knowledge of the fluctuation of several physical quantities: voltage and field fluctuations, (1, 2, 7–9, 16), dipole moment, (8, 9, 17), pH, charge, (18), and the polarizabity and dielectric dispersion of molecular systems (8, 17). In the present article, we estimate the electrical capacitance of several small systems and discuss the implication of its magnitude in the values of several physical fluctuating quantities.

THE ELECTRICAL CAPACITANCE

The Fluctuation–Dissipation Theorem

The timescale of the mentioned processes is in the μs–ns range, hence, we can make use of the fluctuation–dissipation theorem (FDT) in the classical limit ($kT \gg \hbar\omega$ or $\omega \ll kT\hbar^{-1} = 4 \times 10^{13}\text{s}^{-1}$) (8[a],15), namely (see APPENDIX for demonstration).

$$\left\langle (\Delta x)^2 \right\rangle^{\frac{1}{2}} \left\langle (\Delta f)^2 \right\rangle^{\frac{1}{2}} = kT \tag{1}$$

where $\langle (\Delta x)^2 \rangle^{\frac{1}{2}}$ is the square root of the mean square of the spontaneous fluctuations of a quantity x, as due to the action of some random force f senses by the environment, whose corresponding square root of the mean square of the fluctuations is $\langle (\Delta f)^2 \rangle^{\frac{1}{2}}$.

To simplify the notation, we rewrite Eq. 1 as

$$\delta x \cdot \delta f = kT \tag{2}$$

This equation shows a constant equilibrium between the system and the environment, when δf increases in the ambient, the system reacts in such a way as to inhibit the fluctuation of the corresponding physical quantity x and vice versa in order to mantain the product constant equal to kT. We also observe that the product $x \times f$ has dimension of energy.

Capacitance Definition

As an example of Eq. 2, we can consider in a capacitor the relation between the statistical fluctuation of charge, δq, and the corresponding fluctuation of potential, $\delta\psi$, sensed by the environment

$$\delta q \cdot \delta\psi = kT \tag{3}$$

We can define the capacitance as

$$\mathbb{C} = \frac{\delta q}{\delta\psi} \Rightarrow \delta q = \mathbb{C} \cdot \delta\psi \tag{4}$$

From Eqs. 3 and 4, we obtain the following relations

$$\mathbb{C} = \frac{(\delta q)^2}{kT} \qquad \delta\psi = \left(\frac{kT}{\mathbb{C}}\right)^{\frac{1}{2}} \qquad \delta q = (kT \cdot \mathbb{C})^{\frac{1}{2}} \tag{5}$$

[a] In this reference, we used the notation x for Δx.

Encyclopedia of Surface and Colloid Science

Table 1 Potential, electric field, and charge fluctuations as related to given values and sizes of the capacitors (From Ref. 15)

$\mathbb{C}$	$d = \mathbb{C}/(\varepsilon\varepsilon_o)$	$\delta\psi$	$\delta E = (\delta\psi)/d$	$(\delta q)/e_o$
1. pF	1.4 mm	64. μV	46. $\frac{\text{mV}}{\text{m}}$	402.
1. fF	1.4 μm	2. mV	1.4 $\frac{\text{kV}}{\text{m}}$	13.
100. aF	1400. Å	6. mV	43. $\frac{\text{kV}}{\text{m}}$	4.
10. aF	140. Å	20. mV	1.4 $\frac{\text{MV}}{\text{m}}$	1.3
$\frac{(e_o)^2}{kT} = 6.2$ aF	87. Å	26. mV	9.6 $\frac{\text{MV}}{\text{m}}$	1
1. aF	14. Å	64. mV	46. $\frac{\text{MV}}{\text{m}}$	0.4

Cubic capacitor: $\mathbb{C} = (A/d)\varepsilon\varepsilon_o$, $A = d^2$, $\varepsilon = 80$, aF $\equiv$ atto, F $= 10^{-18}$F.

These relations have already been used by several authors in various situations (1, 2, 7–9, 16–18).

The SI system of units is employed throughout this article, namely: ε_o is the permittivity of vacuum ($\varepsilon_o = 8.85 \times 10^{-12}\,\text{C}^2\text{N}^{-1}\text{m}^{-2}$), ε is the dielectric constant of the medium ($\varepsilon = 80$), e_o is the proton charge ($e_o = 1.602 \times 10^{-19}$ C), k is Boltzmann constant ($k = 1.381 \times 10^{-23}$ J/K), T is the absolute temperature.

In Table 1, the relations of Eq. 5 are shown numerically. From the third and fourth column, we can observe the increase of potential and field fluctuations with the decrease of the capacitor value and size. The fifth column shows the diminution of charge fluctuations (number of elementary charges) with the corresponding decrease of the capacitor value and size. The minimum capacitance value at room temperature supporting one elementary charge fluctuation is

$$\frac{(e_o)^2}{kT} = 6.2 \text{ aF},$$

which corresponds to a cubic capacitor in water of side $d = 87$ Å. Inside vesicular biological systems in water with sizes approximately lower than this, charge fluctuations are fractions of one elementary charge (see discussion on this subject in (18)). Biological polyelectrolyte systems have the property of storing a great amount of charge in a small volume (great electrical capacitance). Consequently, the electrical fluctuations are smaller than the example of the cubic capacitor. For example (8), a DNA molecule of 7800 Å (4627 charged groups) has an electrical capacitance of 133 pF ($\delta E = 1687$ V m^{-1}).

Next, we analize the capacitance of various capacitors that appear in polyelectrolytes, and colloidal and vesicular biological systems and the corresponding influence in the electrical fluctuations.

ELECTRICAL FLUCTUATIONS AROUND A CHARGED COLLOID OR MACROION IN AN ELECTROLYTE

Spherical Charged Colloidal System

In this section, we will derive equations valid for the following two systems:

a. A solution of spherical charged particles[b] of radii a immersed in a symmetrical electrolyte solution of point ions (Fig. 1A).
b. A symmetrical electrolyte solution whose ions have a mean radius a (Fig. 1B).

[b] It can also be polyelectrolytes.

A

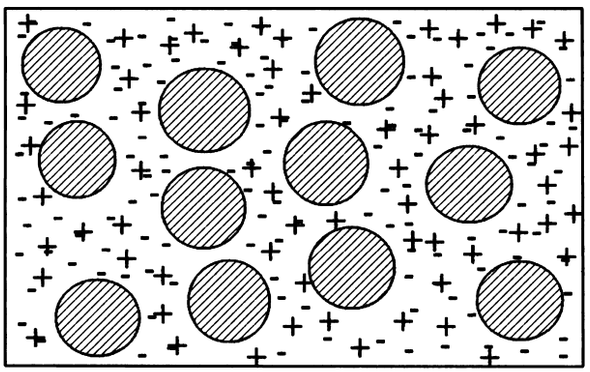

B

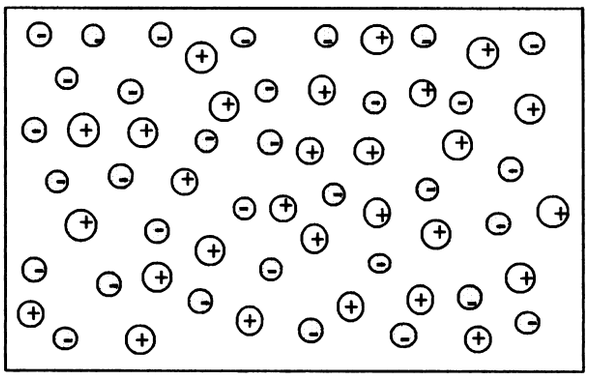

Fig. 1 (**A**) Spherical charged particles of radii a immersed in a symmetrical electrolyte solution of point ions. (**B**) Symmetrical electrolyte solution of ions having a mean radius a. (From Ref. 7.)

The Debye-Hückel theory (19) for a symmetrical electrolyte of valence z with n ions per m^3 gives for the potential, (r) surrounding an spherical particle of charge Q

$$\psi(r) = \frac{Q}{4\pi\varepsilon\varepsilon_o}\frac{e^{\kappa a}}{1+\kappa a}\frac{e^{-\kappa r}}{r} \tag{6}$$

a is the particle radius and κ, called the *Debye-Hückel reciprocal length* parameter, is given by

$$\kappa^2 = \frac{e_0^2}{\varepsilon\varepsilon_o kT}\sum \eta_{i0} z_i^2 = \frac{2000 e_0^2 N_A}{\varepsilon\varepsilon_o kT}\left[\frac{1}{2}\sum c_i z_i^2\right] \tag{7}$$

where η_{i0} and c_i are the number of ions per m^3 and the concentration in moles/liter of ion specie i far away from the surface. The quantity

$$I = \frac{1}{2}\sum c_i z_i^2$$

quantifies the charge in an electrolyte solution and is called the *ionic strength* after Lewis and Randall (20). In case of a solution of a symmetrical $(z{-}z)$ electrolyte, we have

$$\kappa^2 = \frac{2(e_0 z)^2}{\varepsilon\varepsilon_o kT} n = \frac{2(e_0 z)^2}{\varepsilon\varepsilon_o kT} N_A c 10^3 = 8\pi z^2 l_B N_A c 10^3 \tag{8}$$

where N_A is Avogadro constant, c is the solution concentration in moles/liter, and l_B (*Bjerrum length*) is the distance at which the Coulombic energy is equal to kT (l_B = 7.13 Å at 25°C in water) namely

$$l_B = \frac{e_0^2}{4\pi\varepsilon\varepsilon_o kT} \tag{9}$$

Eq. 6 is limited to solutions in which the ratio of the electrical to the thermal energy of the ions is small, namely

$$\frac{z e_0 \psi(r)}{kT} \ll 1 \tag{10}$$

At the particle surface, $r = a$, then

$$\psi(a) = \frac{Q}{4\pi\varepsilon\varepsilon_o a}\frac{1}{1+\kappa a} = \frac{Q}{4\pi\varepsilon\varepsilon_o a} - \frac{Q}{4\pi\varepsilon\varepsilon_o}\frac{\kappa}{1+\kappa a} \tag{11}$$

The first term on the right-hand side of Eq. 11 is the potential ψ_Q at the surface of the particle solely due to the charge on the particle itself. The second term is the portion ψ_{cloud} of the total potential that is due to the arrangement of the surrounding ions in the neighborhood of the particle and is called the *potential of the ionic atmosphere*. The contribution of the cloud to the potential can be written as

$$\psi_{\text{cloud}}(r) = \frac{Q}{4\pi\varepsilon\varepsilon_o r}\left[\frac{e^{\kappa(a-r)}}{1+\kappa a} - 1\right] = \frac{-Q}{4\pi\varepsilon\varepsilon_o \mathbf{x}} \tag{12}$$

with $\mathbf{x}$ given by

$$\mathbf{x} = \frac{r(1+\kappa a)}{1+\kappa a - e^{\kappa(a-r)}} \tag{13}$$

Ionic Cloud Capacitance

The electric charge is distributed in the ionic atmosphere with charge density ρ, then each spherical thin shell has an excess charge $dq = \rho 4\pi r^2 dr$. Because of the spherical symmetry, we tranformed the ionic atmosphere into a thin spherical shell with a charge $-Q$ placed at a distance $\mathbf{x}$ from the site of the central ion. In this way, the central particle or ion and the shell constitute a capacitor, see Fig. 2.

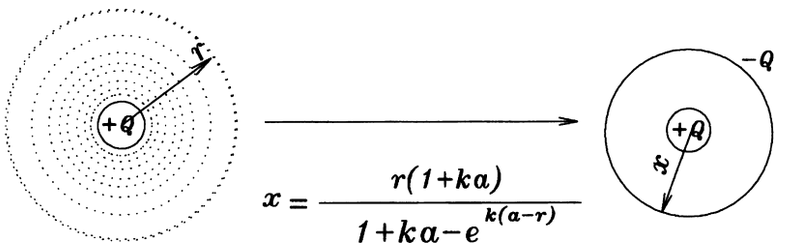

Fig. 2 Transformation of the central ion together with its ionic atmosphere into a capacitor. (From Ref. 7.)

For calculating the capacitance, we need to compute the difference of potencial of the ionic atmosphere between the surface of the particle or ion, $\mathbf{x}(a)$, and $\mathbf{x}(r)$, namely

$$\psi_{\text{cloud}}(a) - \psi_{\text{cloud}}(r) = \frac{-Q}{4\pi\varepsilon\varepsilon_0 r} \times \left[\frac{-1 + \kappa(r-a) + e^{\kappa(a-r)}}{1+\kappa a}\right] \tag{14}$$

The corresponding ionic cloud capacitance will be

$$\mathbb{C}(r) = \frac{Q}{\psi_{\text{cloud}}(a) - \psi_{\text{cloud}}(r)} \tag{15}$$

namely

$${}^{\text{sphere}}\mathbb{C}^{\text{DH}}(r) = \frac{4\pi\varepsilon\varepsilon_0 r(1+\kappa a)}{-1+\kappa(r-a)+e^{\kappa(a-r)}} \tag{16}$$

The usefulness of Eq. 16 is that it allows us to estimate the electrical fluctuations of the system as a function of the distance from the particle.

The ionic cloud capacitance for $r \to \infty$, is given by

$${}^{\text{sphere}}\mathbb{C}^{\text{DH}}_{\infty} = \frac{Q}{\psi_{\text{cloud}}(a)} = 4\pi\varepsilon\varepsilon_0(a+\kappa^{-1}) \tag{17}$$

The entire charge of the ionic atmosphere, $-Q$, given by Eq. 17, can be considered as it is placed on a thin spherical shell at a distance $x = a+\kappa^{-1}$ from the center of the particle.

In the case that the Debye-Hückel approximation Eq. 10 is not longer valid, we have to numerically solve the Poisson-Boltzmann (P-B) equation and use the following equation for the spherical ionic cloud capacitance

$${}^{\text{sphere}}\mathbb{C}(r) = Q\left[\psi_{\text{PB}}(r) - \psi_{\text{PB}}(a) + \frac{Q}{4\pi\varepsilon\varepsilon_0}\left(\frac{1}{a}-\frac{1}{r}\right)\right]^{-1} \tag{18}$$

with ${}^{\text{sphere}}\mathbb{C}_{\infty}$ given by

$${}^{\text{sphere}}\mathbb{C}_{\infty} = Q\left[\frac{Q}{4\pi\varepsilon\varepsilon_0 a} - \psi_{\text{PB}}(a)\right]^{-1} \tag{19}$$

For details of the numerical integration of P-B in cylindrical and spherical systems, see Refs. 9, 15.

Relaxation Time

Suspended charged particles

In this case, we deduce the relaxation time as follows: The central particle practically loses its cloud if it diffuses to a distance λ during relaxation time τ of the fluctuation. In this way, λ is given by

$$\lambda = \tau v_{\text{particle}} = \tau\mu_{\text{particle}}\delta E \tag{20}$$

where v_{particle} and μ_{particle} are the velocity and mobility of the charged particle in solution. The mobility of a particle of charge Q is given by

$$\mu_{\text{particle}} = \frac{Q}{f} = Q\left(\frac{D_{\text{particle}}}{kT}\right) \tag{21}$$

where f ($\text{kg}\cdot\text{s}^{-1}$) is the frictional coefficient of the particle and D_{particle} is its diffusion coefficient (m^2s^{-1}). For a sphere, the frictional coefficient is given by (21)

$$f = 6\pi\eta a \tag{22}$$

As

$$\delta E = \frac{\delta\psi}{\lambda} = \frac{1}{\lambda}\left(\frac{kT}{\mathbb{C}_{\infty}}\right)^{\frac{1}{2}},$$

then from Eq. 20, we have

$$\tau = \frac{\lambda}{\mu_{\text{particle}}\delta E} = \frac{\lambda^2}{\mu_{\text{particle}}}\left(\frac{\mathbb{C}_{\infty}}{kT}\right)^{\frac{1}{2}} \tag{23}$$

For the case of spherical particles in the D-H approximation, $\lambda = \kappa^{-1}$ and $\mathbb{C}_\infty = 4\pi\varepsilon\varepsilon_0(a+\kappa^{-1})$, then Eq. 23, gives

$$\tau = \frac{1}{\kappa^2\mu_{\text{particle}}}\left(\frac{4\pi\varepsilon\varepsilon_0(a+\kappa^{-1})}{kT}\right)^{\frac{1}{2}} \tag{24}$$

Ionic solutions

The ionic relaxation time of the fluctuations can be estimated from the following equation (see, i.e., Reitz and Milford, 1967 (22))

$$\tau = \varepsilon\varepsilon_0\rho \tag{25}$$

with ρ being the solution electrical resistivity.

For solutions of monovalent electrolytes at concentrations 10–100 mM this time is in the nanoseconds range (7).

Method

The method to estimate the electrical fluctuations around a colloidal or polyelectrolyte system in solution, was developed in Ref. 7 and the procedure is as follows:

1. Identification of the molecular-ionic capacitor of the system. The capacitance $\mathbb{C}(r)$ given by Eq. 15.
2. The voltage and field mean square fluctuations are given by

$$\left\langle(\psi_{\text{cloud}}(r)-\psi_{\text{cloud}}(a))^2\right\rangle = \frac{kT}{\mathbb{C}(r)} \tag{26}$$

$$\left\langle(E_r(r))^2\right\rangle = \frac{\left\langle(\psi_{\text{cloud}}(r)-\psi_{\text{cloud}}(a))^2\right\rangle}{r^2} \tag{27}$$

3. The spectral density of the mean square of the fluctuational potential and field are given by

$$\left[(\psi_{\text{cloud}}(r)-\psi_{\text{cloud}}(a))^2\right]_\omega = \frac{2\tau kT}{\mathbb{C}(r)\left[1+(\omega\tau)^2\right]} \tag{28}$$

To center the spectrum in

$$\omega_0 = \frac{2\pi}{\tau},$$

we have to replace $\omega \rightarrow \omega-\omega_0$ in Eq. 28

$$\left[(E_r(r))^2\right]_\omega = \frac{\left[(\psi_{\text{cloud}}(r)-\psi_{\text{cloud}}(a))^2\right]_\omega}{r^2} \tag{29}$$

4. The mean square of the fluctuational potential and field averaged in a time, Δt, are given by

$$\overline{\left\langle(\psi_{\text{cloud}}(r)-\psi_{\text{cloud}}(a))^2\right\rangle}^{t} = \frac{kT}{\mathbb{C}(r)}\left[\frac{\tau}{\Delta t}\right]\left[1-e^{\frac{\Delta t}{\tau}}\right] \tag{30}$$

$$\frac{\overline{\left\langle(\psi_{\text{cloud}}(r)-\psi_{\text{cloud}}(a))^2\right\rangle}^{t}}{r^2} = \frac{\overline{\left\langle(E_r(r))^2\right\rangle}^{t}}{} \tag{31}$$

Ionic Solutions

The electrical mean square fluctuations

Applying Eqs. 16 and 26, we obtain the mean square of the fluctuating potential difference in the DH approximation

$$\left\langle(\psi_{\text{cloud}}(r)-\psi_{\text{cloud}}(a))^2\right\rangle = \frac{kT\left[-1+\kappa(r-a)+e^{\kappa(a-r)}\right]}{4\pi\varepsilon\varepsilon_0 r(1+\kappa a)} \tag{32}$$

The mean square of the field averaged over the distance r is, Eq. 27,

$$\left\langle(E_r(r))^2\right\rangle = \frac{kT\left[-1+\kappa(r-a)+e^{\kappa(a-r)}\right]}{4\pi\varepsilon\varepsilon_0 r^3(1+\kappa a)} \tag{33}$$

Equations for long distances and planar geometry were developed in (7).

The spectral density fluctuations

From Eqs. 16, 25, and 28; we get the spectral density of the mean square of the fluctuational potential

$$\left[(\psi_{\text{cloud}}(r)-\psi_{\text{cloud}}(a))^2\right]_\omega = \frac{kT\rho}{1+(\varepsilon\varepsilon_0\rho\omega)^2}\,\frac{-1+\kappa(r-a)+e^{\kappa(a-r)}}{2\pi r(1+\kappa a)} \tag{34}$$

Correspondingly, the spectral density of the mean square of the fluctuational electric field is given by Eq. 29

$$\left[(E_r(r))^2\right]_\omega = \frac{kT\rho}{1+(\varepsilon\varepsilon_0\rho\omega)^2} \times \frac{-1+\kappa(r-a)+e^{\kappa(a-r)}}{2\pi r^3(1+\kappa a)} \tag{35}$$

The results of these two former equations are a substantial diminution and broadening of the spectrum with increas-

ing concentration and the corresponding diminution of the relaxation time of the fluctuations. Also, an effect of electrical stabilization can be observed, *capacitive effect*, a diminution of the amplitude of the fluctuations with increasing particle size, see spectra in Ref. 7 for a KCl solution.

Spherical Particles

In Fig. 3A and 3B we can observe the mean potential and field fluctuations for different particle sizes immersed in 1-1, 100 mM electrolyte, obtained from Runge-Kutta numerical solution of the P-B equation. The existence of substantial increase in voltage fluctuations is observed with increasing d. We can also observe the capacitive effect, when large particles produce electrical stabilization in their neighborhood. Another result, (7, 9) is that fluctuations are not very sensitive to ionic concentrations for large particles.

Cylindrical Charged Colloidal Particle

We consider a rigid rodlike polyelectrolyte or particule of radius a, with N charged groups and length $L \gg a$, so that end effects may be neglected, then $b = L/N$ is the *linear charge spacing*. The charge Q is distributed uniformly over the surface, with an electrical surface potential ψ_0. The particle is immersed in a solution of pointlike ions of a symmetrical electrolyte of valence z with n ions per m^3.

The contribution of the ionic cloud to the electrostatic potential will be (9)

$$\psi_{\text{cloud}}(r) = \psi(r) + \frac{2kT\xi}{e_0}\ln(r) \tag{36}$$

where $\xi = l_B/b$ is the dimensionless ratio called the *reduced linear charge density* (i.e., a B-DNA molecule has two negative phosphate charges each at a helical spacing of 3.37 Å, then $\xi = l_B/b = 7.13 \times (2/3.37) = 4.23$). Eq. 36 is valid for distances not very far away from the rod surface, $r \ll L$.

Then the ionic cloud capacitance, Eq. 15, is

$${}^{\text{rod}}\mathbb{C}(r) = \frac{L}{l_B}e_0\xi\left[\psi_{\text{PB}}(r) - \psi_{\text{PB}}(a) + \frac{2kT\xi}{e_0}\ln\left(\frac{r}{a}\right)\right]^{-1} \tag{37}$$

where ξ is the reduced linear charge density over the rod surface (9). In this case, the DH approximation (Eq. 10) is valid, then Eq. 37 can be written as

$${}^{\text{rod}}\mathbb{C}_{\text{DH}}(x) = 2\pi L\varepsilon\varepsilon_0\left[\frac{K_0(x) - K_0(x_0)}{x_0K_1(x_0)} + \ln\left(\frac{x}{x_0}\right)\right]^{-1} \tag{38}$$

with ${}^{\text{rod}}\text{C}_{\infty}^{\text{DH}}$ given by (15, 17)

$${}^{\text{rod}}\mathbb{C}_{\infty}^{\text{DH}} = \frac{Q}{\psi_{\text{cloud}}(x_0)} = 2\pi L\varepsilon\varepsilon_0\left[\frac{K_0(x_0)}{x_0K_1(x_0)} + \ln(x_0)\right]^{-1} \tag{39}$$

In general, ${}^{\text{rod}}\mathbb{C}_{\infty}$, is given by

$${}^{\text{rod}}\mathbb{C}_{\infty} = \frac{Q}{\psi_{\text{cloud}}(x_0)} = \frac{4\pi L\varepsilon\varepsilon_0\xi}{y(x_0) + 2z\xi\ln(x_0)} \tag{40}$$

where $y(x_0) = e_0\psi(x_0)/kT$ and $x_0 = \kappa a$ are the dimensionless potential and distance.

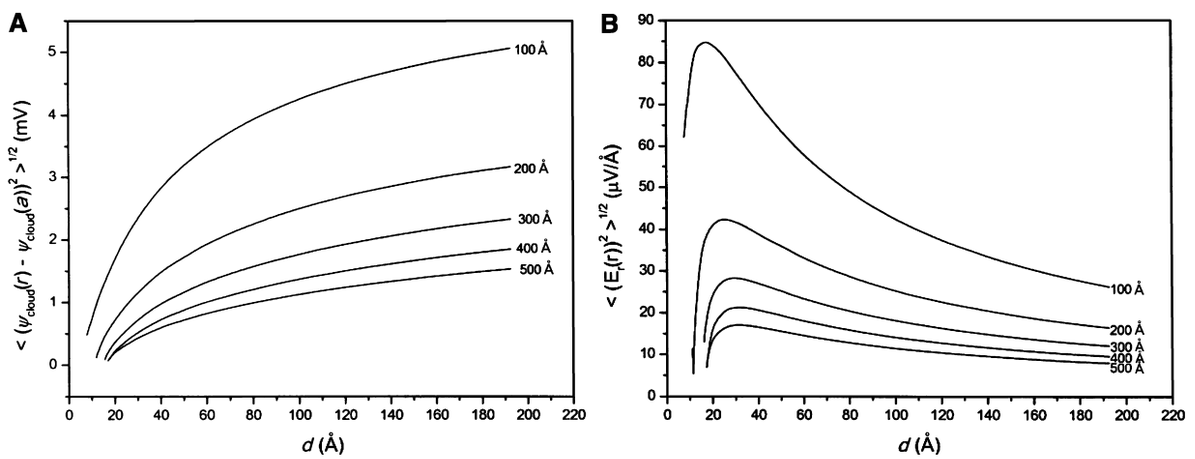

Fig. 3 Mean potential (**A**) and field fluctuations (**B**) for spherical particles with different sizes immersed in 100 mM 1-1 electrolyte in water, obtained from Runge-Kutta numerical solution of the P-B equation, d is the distance from particle surface.

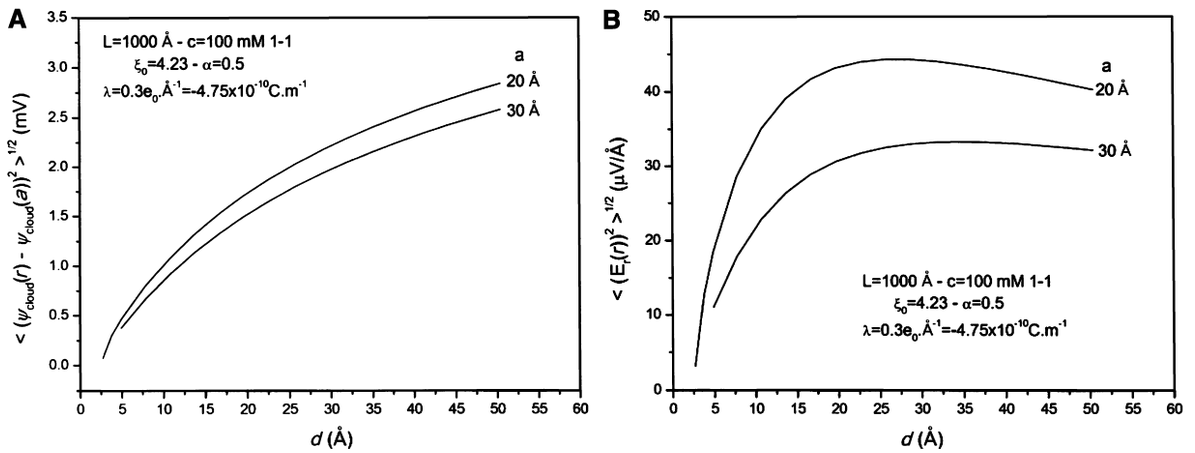

Fig. 4 Mean potential (**A**) and field fluctuations. (**B**) Numerical solutions of the P-B equation for different radii cylindrical polyelectrolytes immersed in 100 mM 1-1 electrolyte in water, d is the radial distance from the cylinder surface.

The thermal electrical fluctuations around charged colloidal cylinders in electrolyte solutions were estimated (9). It was determined that large particles produce electrical stabilization in their neighborhood (capacitive effect). Voltage fluctuations run from 1 to 12 mV, with the corresponding field fluctuations spanning a range of 10 to 400 μV Å^{-1}.

Fig. 4 shows the local electrical fluctuations for cylindrical polyeletrolytes immersed in 100 mM 1-1 electrolyte in water, the voltage fluctuations (A) are in the range (0–3) mV and the corresponding field fluctuations in the (0–40)μV/Å. Eqs. 26, 27, and 37 were used.

Global Electrical Fluctuations

We are sometimes interested in calculating the fluctuations, not as a function of the distance from the particle or ion, but rather the global fluctuations, produced by the whole dissipation of the ionic cloud. This is quite useful when estimating the dielectric relaxation of the system, (8, 17). We have already given an introduction of this when we estimated the relaxation time of suspended charge particles.

In order to estimate the fluctuations of the electric field and dipole moment, we use the derived equations (8, 15). The voltage fluctuation is given by

$$\delta\psi = \left(\frac{kT}{\mathbb{C}}\right)^{\frac{1}{2}} \tag{41}$$

and the field fluctuation by

$$\delta E = \frac{1}{\lambda}\left(\frac{kT}{\mathbb{C}}\right)^{\frac{1}{2}} \tag{42}$$

Correspondingly, the dipole moment fluctuation and the polarizability at zero frequency ($\alpha(0) = \delta p/\delta E$) are given by

$$\delta p = \frac{kT}{\delta E} \qquad \alpha(0) = \mathbb{C}\lambda^2 \tag{43}$$

with λ being the average displacement of the ions under the influence of the thermal fluctuating field, given by Eq. 23

$$\lambda^2 = \tau\mu\left(\frac{kT}{\mathbb{C}}\right)^{\frac{1}{2}} \tag{44}$$

where $\mathbb{C} = \mathbb{C}_\infty$ in the case of global fluctuations of the ionic cloud surrounding a particle or can also be the capacitance $\mathbb{C}_{\text{bound}}$ of the ''bound'' ions in a polyelectrolyte.

The corresponding global spectral density of the mean square of the fluctuational potential and field are given by

$$\left[(\delta\psi)^2\right]_\omega = \frac{2\tau kT}{\mathbb{C}(r)\left[1+(\omega\tau)^2\right]} \tag{45}$$

$$\left[(\delta E)^2\right]_\omega = \frac{\left[(\delta\psi)^2\right]_\omega}{\lambda^2} \tag{46}$$

As an example, we will estimate the global electrical fluctuations of suspended spherical vesicles

Spherical vesicles

Fig. 5 shows a schematic depiction of the system. Table 2 shows the external global fluctuational quantities, obtained by numerically solving the P-B equation, for different sizes bilayer lipid vesicles immersed in 100 mM symmet-

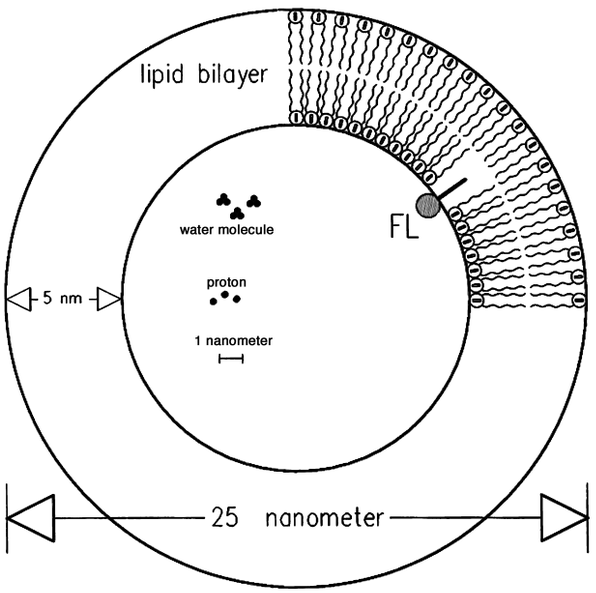

Fig. 5 Schematic draw on approximate scale of a unilamellar vesicle with one membrane fluorescent probe. (From Ref. 18.)

rical monovalent electrolyte (κ^{-1} = 9.63 Å), mantaining the degree of dissociation constant α = 0.3 with the interfacial pK given by (23)

$$pK_a^i = pH + 0.434y_s - \log_{10}\frac{\alpha}{1-\alpha} \tag{47}$$

with the reduced interfacial potential

$$y_s = \frac{e_0\psi_s}{kT}$$

and pH = 7.4, S = 70 Å^2/charged group, correspondingly

$$\sigma = -\left(\frac{e_0}{S}\right)\alpha = -(e_0/70A^2)\times 0.3$$
$$= -6.87\times 10^{-2}\ \text{C.m}^{-2}.$$

We can observe that the obtained values of pK_a^i are in the order of magnitude of the corresponding value of pK_a^i for the group COO^- of the lipid phosphatidylserine.

Fig. 6A and 6B show, for this example, the potential mean squares global fluctuations, Eq. 45, mantaining the concentration of the electrolyte and size of the particles constant, respectively, in both cases σ is constant. We also observe the broadening and diminution of the spectra as particle sizes and concentration increase.

For solving the P-B equation in the interior of the vesicle, we can approximate the surface charge density in the interior surface, σ_{in}, by a variation of the formula given by Israelachvili (24)

$$\sigma_{in} = \sigma_{out}\frac{R_{out}(R_{in}-\kappa_{in}^{-1})}{R_{in}(R_{out}-\kappa_{out}^{-1})} \tag{48}$$

where σ_{out} is the known surface charge density on the outer surface, R_{in}, and R_{out} are the internal and external radii of the vesicle, and κ_{in} and κ_{out} are the Debye-Hückel reciprocal length parameters of the internal and external bathing solutions.

Reverse micelle

In Table 3, $n_{sg} = 4\pi a^2/S$ is the number of surface groups; S = 55 Å^2 is the head groups mean area; $n^+ = \alpha n_{sg}$, in order to preserve the charge neutrality in the microcavite (25, 26), is the number of positive charges in the solution, $n_- = 0.$, $a = 3\ v_w W_0/S$ is the micellar radius (27), v_w = 30 Å^3 is the mean volume of water molecule in the bulk,

$$W_0 = \frac{[H_2O]}{[AOT]}$$

is the molar ratio water:detergent, AOT is the nomenclature for the sodium-di-2ethylhexyl sulphosuccinate; and $c = (n^+/N_A V_m)$, where

$$V_m = \frac{4}{3}\pi a^3$$

is the micellar volume.

Table 2 Parameters and external global fluctuational quantities for bilayer vesicles in solution

a Å	Q_s aC	$\mathbb{C}_\infty$ aF	y_s	ψ_s mV	μ μm^{2}s^{-1}V^{-1}	$\delta\psi$ mV	δE μV/Å	$\delta q/e_0$	$\delta p/p_{H_2O}$	τ^a ps	pK_a^i
100.	− 86.	99.	− 4.61	− 119.	0.46	6.47	671.	4.0	185.	313.	5.77
200.	− 345.	187.	− 5.27	− 136.	0.91	4.70	488.	5.5	254.	215.	5.48
300.	− 776.	274.	− 5.58	− 144.	1.37	3.88	403.	6.6	308.	174.	5.35
400.	− 1381.	362.	− 5.75	− 149.	1.83	3.38	351.	7.6	354.	150.	5.27
500.	− 2157.	449.	− 5.87	− 152.	2.29	3.03	315.	8.5	394.	133.	5.22

[a]We have approximated the cloud average fluctuational displacement $\lambda = \kappa^{-1}$ in Eq. 23.

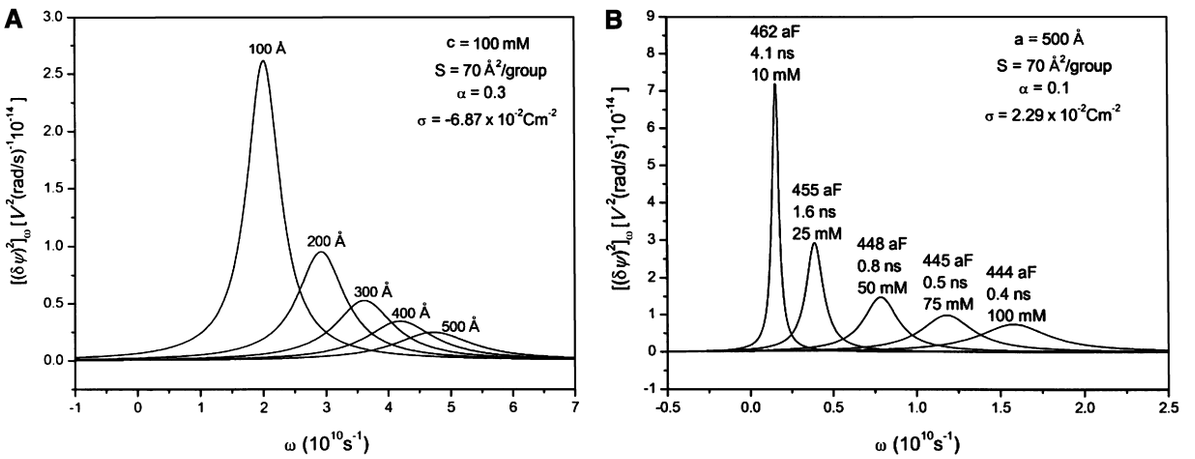

Fig. 6 Potential mean squares global fluctuations obtained from Eq. 45 and by solving the P-B for the exterior of bilayer vesicles immersed in NaCl in water, maintaining the concentration of the electrolyte (**A**) and size of the particles (**B**) constant, respectively. In both cases (**A**) and (**B**), the surface charge density is maintained constant.

The overall charge, $\delta\psi = (kT\mathrm{C})^{\frac{1}{2}}$, voltage,

$$\delta\psi = \left(\frac{kT}{\mathbb{C}}\right)^{\frac{1}{2}},$$

and field,

$$\delta E = \frac{1}{a}\left(\frac{kT}{\mathbb{C}}\right)^{\frac{1}{2}},$$

fluctuations (7, 11) in the micelle, in the reported range of the parameters, are shown in the three last colums of Table 3. $\mathbb{C}$ was calculated in accordance with the following equation

$$\mathbb{C} = \frac{Qe_0}{kT}\frac{1}{y_{\mathrm{cloud}}(a)} = \frac{Qe_0}{kT}\frac{1}{[y_{\mathrm{bare}}(a) - (y(0) - y(a))]} \quad (49)$$

We performed forward integration of the P-B equation, starting at the center of the micelle, with the initial conditions: $y = y(0)$ and $y'(0) = 0.$, varying $y(0)$ until we obtained the value for the first derivative of the reduced potential on the internal surface of the micelle $y'(a) = \sigma e_0/(kT\varepsilon\varepsilon_0\kappa)$.

Cylindrical polyelectrolyte

As an example of global electrical fluctuations, we chose the molecule of DNA. The dielectric dispersion of this molecule, produced by the ionic atmosphere relaxation, was already studied (17). In this case, the relaxation time was approximated by that of the cloud without the polyelectrolyte, $\tau = \varepsilon\varepsilon_0\rho$. In Table 4, the relaxation times were estimated by Eq. 23, which considered the presence of the polyelectrolyte. We can observe that these times are greater than those previously seen (17), because the ions are tighter to the polyion, showing that the approximation $\lambda = \kappa^{-1}$ is a better one.

Fig. 7 shows the potential mean square global fluctuations, Eq. 45 for B-DNA immersed in NaCl solutions in water. We can observe the broadening and diminution of the spectrum with increasing NaCl concentration.

Table 3 Reverse micelle parameters and results from P-B calculations

α	n_{sg}	n^+	c mM	W_o	a Å	σ C m^{-2}	$y(0)$	$y(a)$	$\mathbb{C}$ aF	$\delta q.e_0^{-1}$ ±	$\delta\psi$ mV	δE mV Å^{-1}
0.20	30	6.00	1384	8	13.1	− 0.058	0.806	− 0.586	16.9	1.65	15.6	1.19
0.25	74	18.5	1153	12	19.6	− 0.073	1.194	− 0.897	23.2	1.93	13.4	0.68
0.30	138	41.4	1038	16	26.2	− 0.087	1.538	− 1.186	29.0	2.16	11.9	0.46

Table 4 External global fluctuational parameters for B-DNA in NaCl solution in water. ($\xi_0 = 4.23$, $\alpha = 0.4$, $a = 12.5$ Å, $L = 1000$ Å, $\delta^a = -0.237 \times e_0 Å^{-1}$, $\sigma = -4.84 \times 10^{-2}$ C.m^{-2}, and $\mu = 0.349$ μm^{2}s^{-1}V^{-1})

c mM	κ^{-1} Å	$\mathbb{C}_\infty$ aF	y_s	ψ_s mV	$\delta\psi$ mV	δE μV/Å	$\delta q/e_0$	$\delta p/p_{H_2O}$	τ^b ns	pK_a^i
10	30	516	−5.86	−152	2.83	93	9.1	1335	9.4	5.00
25	19	640	−3.76	−97	2.54	132	10.2	941	4.2	5.94
50	14	590	−2.78	−72	2.65	194	9.8	639	2.0	6.37
75	11	538	−2.34	−60	2.77	249	9.3	498	1.3	6.56
100	10	484	−2.07	−53	2.88	299	9.0	415	0.7	6.68

[a]Linear charge density.
[b]We have approximated the cloud average fluctuational displacement $\lambda = \kappa^{-1}$ in Eq. 23.

ELECTRICAL FLUCTUATIONS ALONG A CHARGED COLLOIDAL CYLINDER IN AN ELECTROLYTE

These fluctuations emerge in rodlike polyelectrolytes in ionic solutions exhibiting longitudinal polarization caused by the ions that, according to a Boltzmann distribution, are more or less trapped on the surface of the polyelectrolyte and form the fraction of the ''bound'' ions. Although they are radially fixed, they still have a certain freedom to move in the longitudinal direction of the molecule. The corresponding capacitance was estimated (8), namely

$$\mathbb{C} = n^2 \frac{(ze_0)^2}{kT} = \left(\frac{\gamma L}{b}\right) \frac{e_0^2}{kT} \tag{50}$$

where n is the number of ''bound'' ions, and $\gamma = zn/N$ is the degree of association of the counterions, z is the valence of the ''bound'' ions, $b = L/N$ is the linear charge spacing, N is the total number of charged polymer sites, and L is the length of the rodlike molecule.

The average displacement λ of the ''bound'' ions is given (8, 29) by,

$$\lambda^2 = \frac{L^2}{12n} \tag{51}$$

The corresponding relaxation time of these fluctuations is

$$\tau = \frac{ze_0 L^2}{12\mu kT} \tag{52}$$

with μ being the mean mobility of the ions along the polymer framework. The lowest relaxation time of fluctuations in counterion density around a long rodlike polyelectrolyte was found to be in the range of 10^{-3} to 10^{-4} sec (Schwarzs (4); Oosawa (6); Takashima (28); Mandel (29).

As an example, we consider DNA molecule with $L = 7800$ Å, $z = 1$, association degree $\gamma = 1$. This molecule has two phosphate negative charges per unit, each with a helical spacing of 3.37 Å, then $b = 3.37$ Å/2 = 1.68 Å, consequently $N = L/b = n = 4643$.

From Eq. 52 and from the experimental value for $\tau = 10^{-3}$ s of Takashima (28), we estimate the mobility μ of the ''bound'' ions as $\mu = 1.96 \times 10^{-9}$ m^{2}s^{-1}V^{-1}, which is 26 times smaller than the mobility of Na ions in water, $\mu^+_{Na} = 5.19 \times 10^{-8}$ m^{2}s^{-1}V^{-1}, showing that these ions are more or less trapped.

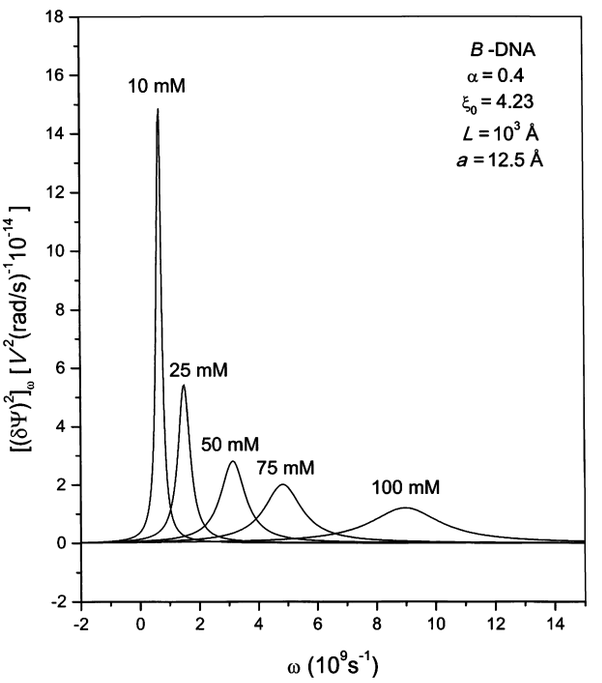

Fig. 7 Potential mean square global fluctuations for *B*-DNA immersed in NaCl in water. Eq. 45 and P-B numerical solution (Table 4).

From Eq. 50, the ''bound'' ions' capacitance is in the order of 134 pF, the corresponding value of $\lambda \sim 33$ Å. The ratio $\delta p{:}p_{H_2O} \sim 4 \times 10^5$ and $\delta E \sim 1681$ V/m, with p_{H_2O} being the permanent dipole moment of water molecule (1.84 D). The relaxation time of these fluctuations are in the order of the ms, which give a dissipated power

$$P = \frac{kT}{2}\frac{1}{10^{-3}} \sim 2. \times 10^{-18}\text{J/s}.$$

This power is in the order of magnitude of that involved in molecular motors (30–33).

ELECTRICAL FLUCTUATIONS IN MEMBRANE SYSTEMS

Biological Ionic Channel

Biological ionic channels are microscopic entities capable of transferring ions at a great rate. Most ion channels exist in one of two basic configurations, namely open or closed. Transitions between channel configurations are mediated by a specialized region of the channel, the gate. Gates can be modulated by chemicals, voltage, or just by being insensitive. In either case, transitions between the various configurations (open, closed, and intermediate states) display a stochastic component, whose nature is poorly understood (Hille (34); DeFelice (35); Lauger (36)).

Cell membranes, on the other hand, are the substratum on which channels insert. Because the membrane matrix is basically electrically insulating and separates two electrolytical media, it acts as an electrical capacitor. Channels, inserted alongside the matrix, can then be viewed as leaks on the membrane dielectric, which leads to the parallel *RC* equivalent for the channel–membrane system (Finkelstein and Mauro (37); De Felice (35)).

In order to determine the voltage fluctuations across cell membranes, the theory of generalized susceptibility was applied (2) to a system consisting of a capacitor and a resistor in parallel, resembling a fragment of biological cell membrane harboring an ionic channel. It appears that for lower channel conductivities, high amplitude voltage fluctuations fall in the range of typical gating response times. It was proposed that voltage fluctuations may be included among the many mechanisms influencing gating behaviour. This model was improved by (38), including solute fluctuations in the cytoplasm due to the movement of ion pairs across the membrane, which affects the frequency spectrum of the electric field but not its mean value.

Noise analysis

The objective of noise analysis is to relate macroscopic observables, such as the mean ionic current $I(t)$ and the current variance $\sigma_I(t)^2$, to microscopic parameters, such as the single-channel current i, the number of functional channels in the membrane N, and the probability that the channels be in the conducting state p.

The experimental data from n current records are

$$I(t) = \frac{1}{n}\sum_{k=1}^{n} y_k(t) \tag{53}$$

$$\sigma_I(t)^2 = \frac{1}{n-1}\sum_{k=1}^{n}[y_k(t) - I(t)]^2 \tag{54}$$

where $y_k(t)$ is the k^{th} membrane current record. For an homogenous population of statistically independent channels, $I(t)$ and $\sigma_I(t)^2$ are related (Ehrenstein, Lecar, and Nossal (39); Begenisich and Stevens (40).

$$I(t) = Nip(t) \tag{55}$$

$$\sigma_I(t)^2 = Ni^2p(t)[1 - p(t)] \tag{56}$$

Eliminating $p(t)$ from Eqs. 55 and 56: gives the expression, introduced by Sigworth (41), that is fitted to the experimental data to yield values for i and N

$$\sigma_I(t)^2 = iI - \frac{I^2}{N} \tag{57}$$

For instance, i = 0.3 pA, and N = 43,000 for the sodium channels in a node of Ranvier. Also, for another important reference on this subject, see Neher and Sakmann (42, 43).

Protonic Fluctuations in Unilamellar Vesicles

Artificial unilamellar vesicles (UV) constitute models in which many transport problems have been studied in recent years (44). The so-called small unilamellar vesicles (SUV) and large unilamellar vesicles (LUV) have been extensively employed to obtain information concerning the passage of different compounds through the cell membrane, such as fatty acids (FA), and have served as vehicles for transport of pharmaceutically relevant substances and, more recently, for genetic materials.

In a recent article (18), we estimated the pH fluctuations in small unilamellar vesicles (SUV) and it was determined that these fluctuations are dependent on such macroscopic variables as pH, pK_a^i, number of buffer groups, v_i, and surface electrical reduced potential y_s. An equation was derived that relates the pH fluctuation and the buffer capacitance C_{buffer}, namely

$$\delta\text{pH} = \frac{e_0}{2.3(kT\mathbb{C}_{buffer})^{\frac{1}{2}}} \tag{58}$$

Table 5 Parameters and surface protonic electrical fluctuations for bilayer vesicles in solution

a Å	Δr Å	$\mathbb{C}_{\text{buffer}}$ fF	y_s	$\delta\psi$ mV	δE μV/Å	$\delta q/e_0$	$\delta p/p_{H_2O}$	δ pH 10^{-2}	Num. Buffers	pK_a^i
100.	3.9	2.33	− 4.61	1.33	343.	19.4	362.	4.5	1795	5.77
200.	3.8	9.37	− 5.27	0.66	175.	38.9	710.	2.2	7181	5.48
300.	3.8	21.0	− 5.58	0.44	117.	58.2	1060.	1.5	16157	5.35
400.	3.8	37.2	− 5.75	0.33	88.	77.4	1412.	1.1	28723	5.27
500.	3.8	58.1	− 5.87	0.27	71.	96.8	1761.	0.9	44880	5.22

with $\mathbb{C}_{\text{buffer}}$ given by

$$\mathbb{C}_{\text{buffer}} = \frac{(\delta q)^2}{kT} = \frac{e_0^2}{kT}\sum_i \frac{\nu_i}{2 + e^{y_s}10^{(\text{pH}-\text{p}K_a^i)} + e^{-y_s}10^{(\text{p}K_a^i-\text{pH})}} \tag{59}$$

where ν_i is the number of buffer groups of type i in the lipid. The relation of $(\delta q)^2$ with $y_s = 0$ coincides with that given by Kirkwood and Schumaker (45), obtained independently using mechanical statistical methods, when they calculated the forces between protein molecules in solution arising from fluctuations in proton charge and configuration.

From our results it was inferred that measurement of pH in small systems has to be performed near the pK of the buffer groups in order that the fluctuational errors be minimized. We showed that pH fluctuations diminish with the increasing size of the SUV and the predicted pH fluctuations decrease as the surface potential becomes less negative as a consequence of decreasing density of charged groups in the inner vesicular surface. It was also predicted that measurable effects will appear on the fluorescence detection due to protonic fluctuations close to the pH-sensing region of the probes.

As an example of the protonic equilibrium at the vesicle surface ($AH \rightleftharpoons A^- + H^+$) we will continue using the example of unilamellar vesicles mentioned in a previous section where we estimated the electrical fluctuations emerging from thermal fluctuations of the external ionic atmosphere surrounding the particle in Table 2. We need to estimate C_{buffer} given by Eq. 59, because it is the link to the knowlege of the electrical thermal fluctuations emerging from this process, as detailed in the following table, Table 5, where Δr is the radial distance between the plates of the equivalent capacitor whose capacitance is $\mathbb{C}_{\text{buffer}}$, namely

$$\Delta r = \frac{4\pi\varepsilon\varepsilon_0 a^2}{\mathbb{C}_{\text{buffer}} - 4\pi\varepsilon\varepsilon_0 a} \tag{60}$$

The superficial $\mathbb{C}_{\text{buffer}}$ (Table 5) is greater than $\mathbb{C}_\infty$ produced by the ionic atmosphere and the charged surface (Table 2). In calculating Δr, we used the dielectric constant of water $\varepsilon = 80$, although water molecules are rather ordered near the surface so that ε can be lower, and, consequently, Δr can also be lower.

Electrical Fluctuations in Molecular Motors

F_1-ATPase

The synthesis of ATP in eukariotic cells occurs at the expense of proton flow driven by the proton-motive force (E_{PMF}) across ATP synthase molecules inserted in the inner mitochondrial membrane (IMM). This enzyme is composed of a membrane-embedded, proton-conducting portion, F_0, and a protruding portion, F_1 (Fig. 8). This system constitute a highly efficient molecular motor that rotates with discrete 120° steps, (46, 47). Proton gradients as high as 1 pH unit can occur at that location (48) and superposition with electrical potential difference can lead to E_{PMF}'s attaining the 200 mV mark.

Because the intermembrane space in most of its traject has a width of only about 10–20 nm, this dimension limits a region of molecular proportions where fluctuations in thermodynamic parameters may become an important part of the forces acting on the molecular machines inserted alongside the inner mitochondrial membrane, see Fig. 8.

The intermembrane mitochondrial space (IMMS) is delimited by the inner and outer mitochondrial membranes and defines a region of molecular dimension where fluctuations of the number of free protons and of transmembrane voltage can give rise to fluctuations in the proton–electromotive force (E_{PMF}) across the inner mitochondrial membrane (IMM).

We have applied (16) the fluctuation–dissipation theorem (FDT) to an electrical equivalent circuit consisting of a resistor (R_m) in parallel with a capacitor (C_m) representing the passive electrical properties of the IMM, in series with another capacitor (C_b), representing the proton buffering power of the IMMS fluid. An access resistance, R_a,

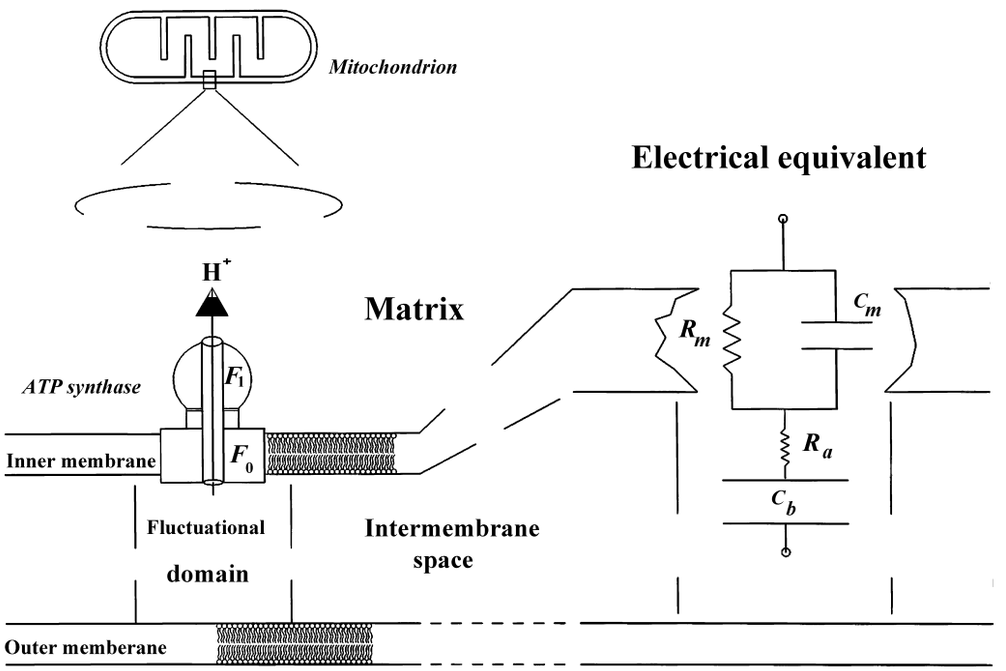

Fig. 8 Diagram showing the mitochondrial membrane and electrical equivalent. (From Ref. 16.)

was defined as a link between the capacitor C_b and the membrane.

Average E_{PMF} fluctuations across the IMM were calculated for different assumptions concerning the intermembrane space dimensions. The calculated average E_{PMF} fluctuations were in the vicinity of 100 mV for relaxation times in the few microseconds range. The corresponding fluctuational protonic free energy is about 10 kJ/mole, which coincides with the binding energy for protons in different transporters. This suggests that fluctuations in E_{PMF} can be of relevance in the universe of forces influencing the molecular machinery embedded in the IMM.

Outer hair cells

As another example, we will estimate the electrical fluctuations of the outer hair cells (OHC) that, in accordance with conducted experiments (49), demonstrate that OHC electromotility is driven by a large number of small independent $\sim 4000/\mu\mathrm{m}^2$ (50, 51) voltage-sensing elementary motors, closely associated with the plasma membrane, whose primary mode of action is longitudinal deformation. It is conceivable that transmembrane voltage gradients produce conformational changes in protein structures associated with the cell's cortex that directly change the longitudinal length of the elementary motor units. Mammalian OHC are slender cylindrical structures of fairly uniform diameter ($\sim 8-10$ μm) and their length ranges from $\sim 20-30$ μm in the high-frequency cochlear base to about $80-100$ μm in the low-frequency apex. A nonlinear charge movement, or corresponding voltage-dependent capacitance, has been observed in this cell and it probably reflects the activity of the motility voltage sensor (50, 52–54). In this section, we estimate the electrical fluctuations in the OHC from the experimental results for the capacitance and relaxation times (50). In this case, the experimental data for the voltage-dependent capacitance and charge movement associated with the system of membrane motors are fitted by the following equations

$$C_{(v)} = Q_{\max}\frac{ze_0}{kT}\left\{\left[1+\exp\left(-\frac{ze_0}{kT}(\mathrm{V}-\mathrm{V}_h)\right)\right]^2 \times \exp\left[\frac{ze_0}{kT}(\mathrm{V}-\mathrm{V}_h)\right]\right\}^{-1} \tag{61}$$

$$Q_{(v)} = Q_{\max}\left\{1+\exp\left[\frac{ze_0}{kT}(\mathrm{V}-\mathrm{V}_h)\right]\right\}^{-1} \tag{62}$$

In Fig. 9, these two equations, for given values of the parameters $Q_{\max}$, V_h, and z, are represented.

Because of the high values of the capacitance of this system, the voltage and field fluctuations are not so high, correspondingly high dipole moment fluctuations ($\delta p = kT/\delta E$) appear across the OHC's basolateral membrane (across the motors), the electrical noise is measurable and

pausible of analyzing in order to obtain additional information which may help reveal mechanisms at a molecular level (55). It is estimated that OHC motility in the (16–18)kHz range, where measurements are available, is about 20% of basilar membrane motion (56). The receptor potential is attenuated at high frequencies due to the $RC_{(v)}$ filtering of the cell membrane. Dallos and Evans (56) proposed that the effective electrical stimulus that powers the OHC motile response at high frequencies is not the cell's own receptor potential, but an extracellular voltage gradient, established across the hair cell, between the scala media and intraorgan of Corti fluid spaces; for a 20 μm (basal) cell, this basolateral membrane voltage is estimated to be $\sim$22 μV, producing an electromotile displacement of $\sim$0.11 nm at the behavioral threshold. At this same level, basilar membrane displacement is $\lambda \sim 0.16$ nm (57); this means that we have a polarizability, Eq. 43, $\alpha(0) = C\lambda^2 = 5.1\times10^{-31}$F m^2 for a membrane with a capacitance of 20 pF, this static polarizability is 3.2×10^9 greater than the mean polarizability of water molecule $\overline{\alpha_{H_2O}} = 1.6 \times 10^{-40}$F m^2, correspondingly we have a mean fluctuational dipole moment across the lateral basal membrane at room temperature $\delta p = [\alpha(0)kT]^{1/2} = 4.6 \times 10^{-26}$ C m $= 1.48 \times 10^4$ D, which is 7.5×10^3 greater than the permanent dipole moment of a water molecule (1.84 D). The thermal fluctuating field for this case is $\delta E = kT/\delta p = 9 \times 10^4$ V m^{-1} = 9 μV Å^{-1}, 10 times smaller than the fluctuational fields surrounding cylindrical polyelectrolytes immersed in electrolyte solutions (9).

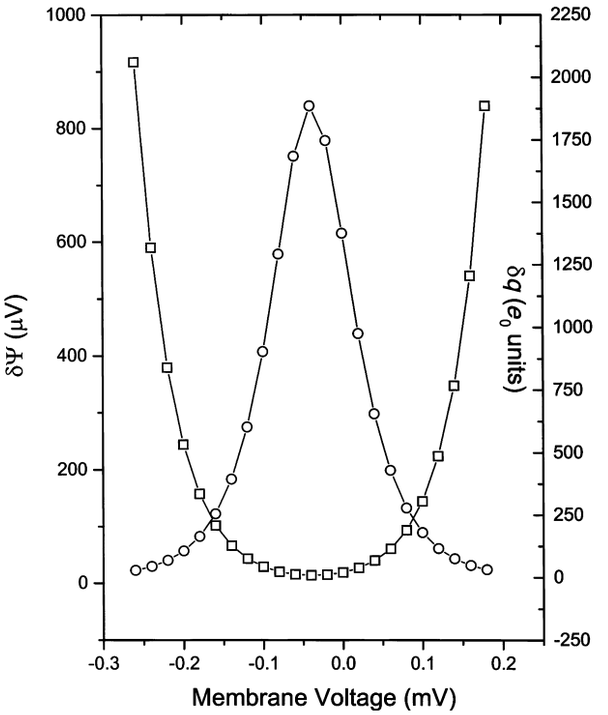

Fig. 10 Potential (- -) and charge fluctuations (-o-) for given values of the membrane applied potential.

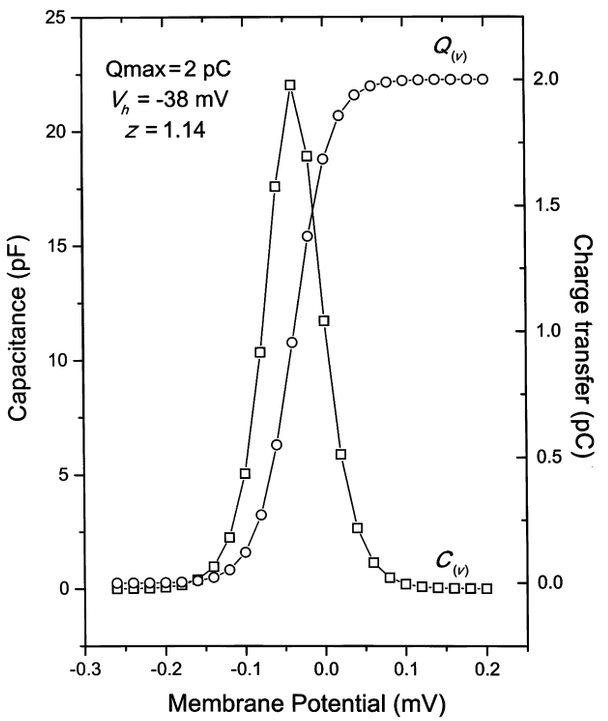

Fig. 9 Representation of Eqs. 61 and 62. (From Ref. 50.)

Fig. 10 spans a wide range of potential and charge fluctuations for given values of the membrane applied potential. Modeling the electric circuit associated with the motor as an $RC_{(v)}$ circuit in parallel (R is the channels electrical resistance). In this circuit, the relation between the Fourier components of the spontaneous thermal fluctuational current I_ω and voltage, V_ω is given by (2)

$$V_\omega = Z(\omega)I_\omega \tag{63}$$

with $Z(\omega)$ given by

$$\frac{1}{Z(\omega)} = \frac{1}{R} + i\omega C_{(v)} \tag{64}$$

the corresponding spectral density of the mean square of the fluctuational voltage $(V^2)_\omega$, and current, $(I^2)_\omega$, with relaxation time $\tau = RC_{(v)}$ are given by

$$(V^2)_\omega = \frac{2\tau kT}{C_{(v)}[1 + (\omega\tau^2)]} \tag{65}$$

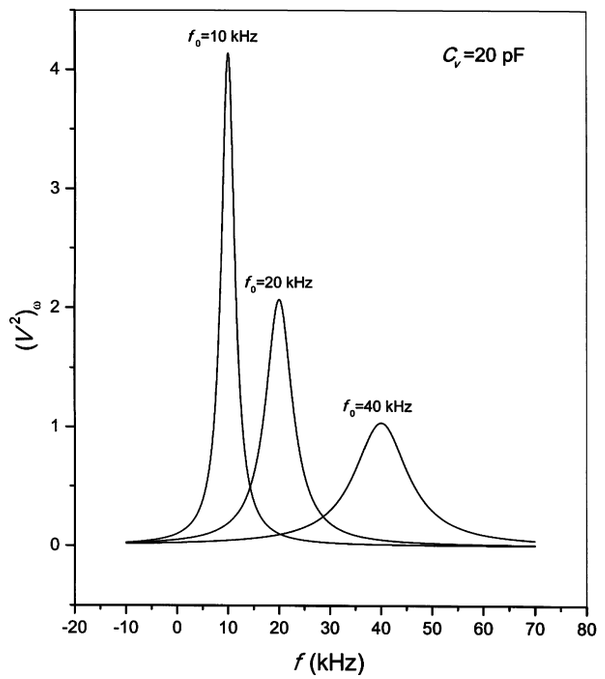

Fig. 11 Spectral density of the mean square of the fluctuational voltage $(V^2)_\omega$, for a given value of the motors capacitance, $C_{(v)} = 20$ pF, and three characteristics frequencies.

and

$$(I^2)_\omega = \frac{(V^2)}{|Z(\omega)|^2} = \frac{2kTC_{(v)}}{\tau} \tag{66}$$

Fig. 11 spans the mean square of the fluctuational voltage, $(V^2)_\omega$, for a given value of the motors capacitance, $C_{(v)} = 20$ pF, and three characteristic frequencies. The dependency of the mean square fluctuational current with frequency depends of the variation of $C_{(v)}$ with frequency. Experimental data on this subject are poor, in one article (50), a slight variation of the capacitance with frequency in the low frequency range is reported.

CONCLUSION

We saw that thermal electrical fluctuations in small systems are the origin of many physical-chemistry phenomena, consequently, they give information of the system parameters: polarizability of colloids and polyelectrolytes in ionic solutions, buffering power of solutions, single-channel current *i*, and number of functional channels in the membrane *N*. For example, from the knowlege of the experimental data for the spectral density of the mean square of the fluctuational potential, $(V^2)_\omega = \sigma_V(\omega)^2$, and current, $(I^2)_\omega = \sigma_I(\omega)^2$, we can obtain information of the system parameters as *R* and *C*.

Molecular systems are sufficiently small and fast as to both sense and respond to local fluctuating electrical fields (Läuger (36); Hille (34) or for an efficient processing of information in the form of fast conformational changes (58). To explain any possible mechanism at the molecular level, which involves an electric process, fluctuations have to be considered. How these fluctuations are coupled to the biological machine remains an open question.

ACKNOWLEDGMENTS

This work was partially supported by the Conselho Nacional de Desenvolvimento Científico e Tecnológico (CNPq-Brazil). The author also wants to express his gratitude to Dr. Arthur Hubbard for inviting him to participate in this Encyclopedia.

APPENDIX

FLUCTUATION–DISSIPATION THEOREM

One way of formulating the FDT[c] is by formally regarding the spontaneous fluctuations of a quantity *x* as due to the action of some random force *f*, meaning that the environment senses the system through the generalized susceptibility $\alpha(\omega)$, and responds with a fluctuating force. The Fourier components x_ω and f_ω are related by

$$x_\omega = \alpha(\omega) f_\omega \tag{A–1}$$

The relation between the generalized impedance $Z(\omega)$ and $\alpha(\omega)$ is

$$Z(\omega) = -\frac{1}{i\omega\alpha(\omega)} \tag{A–2}$$

with *i* being the imaginary unit. As $x_\omega = x_{0\omega}\, e^{-i\omega t}$, we can write

$$f_\omega = Z(\omega)\frac{dx_\omega}{dt} \tag{A–3}$$

The spectral densities of the fluctuation are given by

$$(x^2)_\omega = |\alpha(\omega)|^2 (f^2)_\omega \tag{A–4}$$

The results of the FDT are

$$(x^2)_\omega = \hbar\alpha''(\omega) coth \frac{\hbar\omega}{2kT} \tag{A–5}$$

[c] We use *x* for Δx to simplify the equations.

Correspondingly

$$(f^2)_\omega = \frac{\hbar\alpha''(\omega)}{|\alpha(\omega)|^2} coth \frac{\hbar\omega}{2kT} \tag{A–6}$$

The mean square of the fluctuating quantity is

$$\begin{aligned} <x^2> &= \frac{1}{\pi}\int_0^\infty (x^2)_\omega d\omega \\ &= \frac{\hbar}{\pi}\int_0^\infty \alpha''(\omega) coth\frac{\hbar\omega}{2kT} d\omega \end{aligned} \tag{A–7}$$

These formulas constitute the FDT, established by Callen and Welton (59) They relate the fluctuations of physical quantities to the dissipative properties of the system. At energies $kT \gg \hbar\omega$ (classical limit $\omega \ll 4.10^{13}\mathrm{s}^{-1}$), we have $\coth(\hbar\omega/2kT) \approx 2kT/\hbar\omega$, and $|\alpha(\omega)|^2 \approx |\alpha'(0)|^2$. Then Eq. A–7 becomes

$$<x^2> = \frac{2kT}{\pi}\int_0^\infty \frac{\alpha''(\omega)}{\omega} d\omega = kT|\alpha'(0)| \tag{A–8}$$

Where we used the Kramers and Kronig's relations (1927; 60)

Analogously

$$\begin{aligned} <f^2> &= \frac{1}{\pi}\int_0^\infty (f^2)_\omega d\omega \\ &= \frac{2kT}{\pi|\alpha'(0)|^2}\int_0^\infty \frac{\alpha''(\omega)}{\omega} d\omega \\ &= \frac{kT}{|\alpha'(0)|} \end{aligned} \tag{A–9}$$

From Eqs. A–8 and A–9, we obtain (8)

$$<x^2><f^2> = (kT)^2 \tag{A–10}$$

This is the classical analogy of the Heisenberg uncertainty principle.

Examples of Eqs. 2 and A-10 are the following relations

$$\begin{aligned} \delta q \cdot \delta\psi &= kT \\ \delta p \cdot \delta E &= kT \\ \delta V \cdot \delta P &= kT \\ \delta A \cdot \delta\Pi &= kT \end{aligned} \tag{A–11}$$

In the first relation of the former, Eq. A-11, δq can be the statistical fluctuation of charge produced in a capacitor as due to the action of some random potential ψ sensed by the environment whose statistical fluctuation is $\delta\psi$. In the second relation, p is the dipole moment and E is the electric field, in the third relation, V is the volume and P is the pressure, and in the fourth relation, A is the area per molecule and Π is the surface pressure ($\mathrm{N}\cdot\mathrm{m}^{-1}$) in a Langmuir-Adam surface balance.

Electric Circuit

As an example, we consider an electric circuit, where the relation between the Fourier components of the spontaneous fluctuational current I_ω and voltage V_ω is given by

$$V_\omega = Z(\omega) I_\omega \tag{A–12}$$

Eq. A-1 can be written as

$$q_\omega = \alpha(\omega) V_\omega \tag{A–13}$$

where q_ω is the Fourier component of the fluctuational charge. In case of a *RC* circuit in serie, we have

$$Z(\omega) = R + \frac{1}{i\omega C} \tag{A–14}$$

Correspondingly, from Eqs. A-2 and A-14, $\alpha(\omega)$ is given by

$$\alpha(\omega) = \frac{-C}{1+(\tau\omega)^2} + i\frac{\tau\omega C}{1+(\tau\omega)^2} \tag{A–15}$$

Then

$$\alpha'(\omega) = \frac{-C}{1+(\tau\omega)^2},\ \alpha''(\omega) = \frac{\tau\omega C}{1+(\tau\omega)^2} \tag{A–16}$$

From Eqs. A-13 and A-16, and considering the classical limit, we obtain

$$(q^2)_\omega = \frac{2kT\tau C}{1+(\tau\omega)^2} \tag{A–17}$$

and

$$(V^2)_\omega = \frac{2kT\tau}{C\left(1+(\tau\omega)^2\right)} \tag{A–18}$$

Then, from Eq. A-8

$$<q^2> = \frac{1}{\pi}\int_0^\infty (q^2)_\omega \quad d\omega = kTC \tag{A–19}$$

Correspondingly, the mean quadratic fluctuation of the voltage, $<V^2> = <q^2> C^{-2}$, will be

$$<V^2> = \frac{kT}{C} \tag{A–20}$$

REFERENCES

1. Weaver, J.C.; Astumian, R.D. The response of living cells to very weak electric-fields-the thermal noise limit. Science **1990**, *247*, 459–462.
2. Procopio, J.; Fornés, J.A. Fluctuation-dissipation theorem imposes high-voltage fluctuations in biological ionic channels. Phys. Rev. E: Sta. Phys., Plasmas, Fluids, Relat. Interdiscip. Top. **1995**, *51*, 829–831.
3. Kirkwood, J.G.; Shumaker, J.B. The influence of dipole moment fluctuations on the dielectric increment of proteins in solution. Proc. Natl. Acad. Sci. U.S.A. **1952**, *38*, 855–862.
4. Schwarz, G. A theory of the low-frequency dielectric dispersion of colloid particles in electrolyte solution. J. Phys. Chem. **1962**, *66*, 2636–2642.
5. Oosawa, F. Counterion fluctuation and dielectric dispersion in linear polyelectrolytes. Biopolymers **1970**, *9*, 677–688.
6. Oosawa, F. *Polyelectrolites, Chap. 5*; Marcel Dekker: New York, 1971.
7. Fornés, J.A. Electrical fluctuations in colloid and ionic solutions. J. Colloid Interface Sci. **1997**, *186*, 90–101.
8. Fornés, J.A. Fluctuations-dissipation theorem and the polarizability of rodlike polyelectrolytes: an elelectric circuit view. Phys. Rev. E: Sta. Phys., Plasmas, Fluids, Relat. Interdiscip. Top. **1998**, *57*, 2110–2114.
9. Fornés, J.A. Thermal electrical fluctuations around a charged colloidal cylinder in an electrolyte. Phys. Rev. E: Stat. Phys., Plasmas, Fluids, Relat. Interdiscip. Top. **1998**, *57*, 2104–2109.
10. Astumian, R.D.; Bier, M. Fluctuation driven ratchets—molecular motors. Phys. Rev. Lett. **1994**, *72*, 1766–1769.
11. Oosawa, F. Field fluctuation in ionic solutions and its biological significance. J. Theor. Biol. **1973**, *39*, 373–386.
12. Schurr, J.M. Theory of quasi elastic light scattering from chemically reactive ionic solutions. J. Phys. Chem. **1969**, *73*, 2820–2828.
13. Schurr, J.M. Dielectric dispersion of linear polyelectrolytes. Biopolymers **1971**, *10*, 1371–1375.
14. Chandler, D.; Andersen, H. Mode expansion in equilibrium statistical mechanics. II. A rapidly convergent theory of ionic solutions. J. Chem. Phys. **1971**, *54*, 26–33.
15. Fornés, J.A. The electrical capacitance of small systems. J. Colloid Interface Sci. **2000**, *226*, 172–179.
16. Procopio, J.; Fornés, J.A. Fluctuations of the proton-electromotive force across the inner mitochondrial membrane. Phys. Rev. E: Sta. Phys., Plasmas, Fluids, Relat. Interdiscip. Top. **1997**, *55*, 6285–6288.
17. Fornés, J.A. Dielectric relaxation around a charged colloidal cylinder in an electrolyte. J. Colloid Interface Sci. **2000**, *222*, 97–102.
18. Fornés, J.A.; Ito, A.S.; Curi, R.; Procopio, J. pH Fluctuations in unilamellar vesicles. Phys. Chem. Chem. Phys. **1999**, *1* (22), 5133–5138.
19. Debye, P.; Hückel, E. Theory of electrolytes. Part I. Freezing-point depression and cognate phenomena. Part II. Law of the limit of electrolytic conductivity. Phys. Z. **1923**, *24*, 185–206, 305–325.
20. Lewis, G.N.; Randall, M. The activity coefficient of strong electrolytes. J. Am. Chem. Soc. **1921**, *43*, 1112–1154.
21. Van Holde, K.E. *Physical Biochemistry*; Prentice-Hall, Inc.: Englewood Cliffs, New Jersey, 1971; 81.
22. Reitz, J.R.; Milford, F.J. *Foundations of Electromagnetic Theory*; Addison-Wesley Publishing Company, Inc.: Menlo Park, California, 1967; 139, Eq. 7.
23. Tanford, C. The interpretation of hydrogen ion titration curves of proteins. Adv. Protein Chem. **1962**, *17*, 69–165.
24. Israelachvili, J.N. Theoretical considerations on the asymmetric distribution of charged phospholipid molecules on the inner and outer layers of curved bilayer membranes. Biochim. Biophys. Acta **1973**, *323*, 659–663.
25. Zhou, Y.; Stell, G. Fluids inside a pore–an integral equation approach III. Water-in-oil microemulsions. Mol. Phys. **1989**, *68*, 1265–1275.
26. Bratko, D.; Luzar, A.; Chen, S.H. Electrostatic model for protein/reverse micelle complexation. J. Chem. Phys. **1988**, *89*, 545–550.
27. Karpe, P.; Ruckenstein, E. Effect of hydration ratio on the degree of counterion binding and pH distribution in reverse micelles with aqueous core. J. Colloid Interface Sci. **1990**, *137*, 408–424.
28. Takashima, S. Dielectric dispersion of DNA. J. Mol. Biol. **1963**, *7*, 455–467.
29. Mandel, M. The electric polarization of rod-like, charged macromolecules. Mol. Phys. **1961**, *4*, 489–496.
30. Vale, R.D.; Oosawa, F. Protein motors and Maxwell's demons: does mechanochemical transduction involve a thermal ratchet? Adv. Biophys. **1990**, *26*, 97–134.
31. Svoboda, K.; Schmidt, C.F.; Schnapp, B.J.; Block, S.M. Direct observation of kinesin stepping by optical trapping interferometry. Nature **1993**, *365*, 721–727.
32. Svoboda, K.; Block, S.M. Force and velocity measured for single kinesin molecules. Cell **1994**, *77*, 773–784.
33. Astumian, R.D.; Bier, M. Mechanochemical coupling of the motion of molecular motors to ATP hydrolysis. Biophys. J. **1996**, *70*, 637–653.
34. Hille, B. *Ionic Channels of Excitable Membranes*; Sinauer Associates, Inc. Publishers: Sunderland, Massachusets, 1992.
35. DeFelice, L.J. *Introduction to Membrane Noise*; Plenum Press: New York, 1981.
36. Läuger, P. Dinamics of ion transport systems in membranes. Physiol. Rev. **1987**, *67*, 1296–1331.
37. Finkelstein, A.; Mauro, A. *Handbook of Physiology, Section 1: The Nervous System*; Kandel, E.R., Ed.; American Physiological Society: Washington D.C., 1977; Vol. 1, Pt. 1.
38. Fay, J.A. Thermal fluctuations of electric field and solute density in biological cells. Phys. Rev. E: Sta. Phys., Plasmas, Fluids, Relat. Interdiscip. Top. **1997**, *56*, 3460–3467.
39. Ehrenstein, G.; Lecar, H.; Nossal, R. The nature of the negative resistance in bimolecular lipid membranes containing excitability-inducing material. J. Gen. Physiol. **1970**, *55*, 119–133.
40. Begenesich, T.; Stevens, C.F. How many conductance

states do potassium channels have? Biophys. J. **1975**, *15*, 843–846.
41. Sigworth, F.J. The variance of sodium current fluctuations at the node of Ranvier. J. Physiol. **1980**, *307*, 97–129.
42. Neher, C.; Sakmann, B. Single-channel currents recorded from membrane of denervated frog muscle fibres. Nature **1976**, *260*, 799–802.
43. Neher, C.; Sakmann, B. Noise analysis of drug induced voltage clamp currents in denervated frog muscle fibres. J. Physiol. **1976**, *258*, 705–729.
44. Hamilton, J.A. Fatty acid transport: difficult or easy? J. Lipid Res. **1998**, *39*, 467–481.
45. Kirkwood, J.G.; Shumaker, J.B. Forces between protein molecules in solution arising from fluctuations in proton charge and configuration. Proc. Natl. Acad. Sci. U.S.A. **1952**, *38*, 863–887.
46. Yasuda, R.; Hiroyuki, N.; Kinosita, K., Jr.; Yoshida, M. F_1-ATPase is a highly efficient molecular motor that rotates with discrete 120° steps. Cell **1998**, *93*, 1117–1124.
47. Kinosita, K., Jr.; Yasuda, R.; Noji, H.; Ishiwata, S.; Yoshida, M. F_1-ATPase: a rotary motor made of a single molecule. Cell **1998**, *93*, 21–24.
48. Lehninger, A.L.; Nelson, D.L.; Cox, M.M. *Principles of Biochemistry*; Worth Publishers, Inc.: New York, 1993.
49. Dallos, P.; Evans, B.N.; Hallworth, R. Nature of the motor element in electrokinetic shape changes of cochlear outer hair cells. Nature **1991**, *350*, 155–157.
50. Santos-Sacchi, J. Reversible inhibition of voltage-dependent outer hair cell motility and capacitance. J. Neurosci. **1991**, *11*, 3096–3110.
51. Kalinec, F.; Holley, M.C.; Iwasa, K.H.; Lim, D.J.; Kachar, B. A membrane-based force generation mechanism in auditory sensory cells. J. Proc. Natl. Acad. Sci. USA. **1992**, *89*, 8671–8675.
52. Ashmore, J.F. *Mechanics of Hearing*; Kemp, D., Wilson, J.P., Eds.; Plenum: New York, 1989; 107–113.
53. Ashmore, J.F. *Sensory Transduction*; Borselino, A., Cervetto, L., Torre, V., Eds.; Plenum: New York, 1990; 25–50.
54. Santos-Sacchi, J. *The Mechanics and Biophysics of Hearing*; Dallos, P., Geisler, C.D., Mathews, J.W., Ruggero, M.A., Steele, C.R., Eds.; Springer: Berlin, 1990; 69–75.
55. Stevens, C.F. Inferences about membrane properties from electrical noise measurements. Biophys. J. **1972**, *12*, 1028–1046.
56. Dallos, P.; Evans, B.N. High-frequency motility of outer hair cells and the cochlear amplifier. Science **1995**, *267*, 2006–2009.
57. Sellick, P.M.; Patuzzi, R.; Johnstone, B.M. Measurement of basilar membrane motion in the guinea pig using the Mössbauer technique. J. Acoust. Soc. Am. **1982**, *72*, 131–141.
58. Fornés, J.A. Information flow to dissipate an ionic fluctuation through a membrane channel. J. Colloid Interface Sci. **1996**, *177*, 411–413.
59. Callen, H.B.; Welton, T.A. Irreversibility and generalized noise. Phys. Rev. **1951**, *83*, 34–40.
60. Landau, L.D.; Lifshitz, E.M. *Statistical Physics*; Pergamon Press: Oxford, 1988; 387.